A Hybrid Stochastic-Neuro-Fuzzy Model-Based System for In-Flight Gas Turbine Engine Diagnostics

Dan M. Ghiocel and Joshua Altmann

STI Technologies
1800 Brighton-Henrietta TL Rd.
Rochester, New York, USA
Ph: (716)424-2010

Abstract: One key aspect when developing a real-time in-flight risk-based health management system for jet engines is the development of accurate and robust fault classifiers. Regardless of the complex uncertainty propagation in the data fusion process, the selection of fault classifiers is the critical aspect of a health management system. The paper illustrates the application of a hybrid *Stochastic-Fuzzy-Inference Model-Based System (StoFIS)* to fault diagnostics and prognostics for both the engine performance. The random fluctuations of jet engine performance parameters during flight missions are modeled using multivariate stochastic models. The fault diagnostic and prognostic risks are computed using a stochastic model-based deviation (using a gas-path analysis model) approach. At any time the engine operation for the future is approached as a conditional reliability problem where the conditional data are represented by the past operational history monitored on-line by the engine health management (EHM) system. To capture the complex functional relationships between different engine performance parameters during flight fast an adaptive network-based fuzzy inference system is employed. This increases significantly the robustness of the EHM system during highly transient in-flight conditions. Both the monitored and fault data uncertainties are considered in a multidimensional parameter space, with two probabilistic-based safety margins employed for fault detection and diagnostic, as follows: (i) Anomaly Detection Margin (ADM) and (ii) Fault Detection Margin (FDM).

Key Words: ANFIS, Engine Health Monitoring, Gas Path Analysis, and Stochastic Analysis

Adaptive Network-based Fuzzy Inference System (ANFIS) GPA Modeling: A schematic model of the investigated turbofan engine, including the performance parameters used for fault diagnostic is shwoimplemented in the ANFIS GPA/Stochastic engine health monitoring system are shown in figure 1. Figures 2 and 3 show pressure variations as a function of the high-pressure shaft speed. It is obvious from these figures that although for slowly varying ground tests the pressure closely follows a non-linear relationship with shaft speed, for in-flight testing the pressure deviates from this non-linear path due to highly transient conditions and changes in the inlet conditions. This means using deviations from a fitted polynomial curve for diagnostics, as commonly used in earlier engine health monitoring software based on ground-test data, is not suited to in-flight conditions. This is the driving force to move towards deviations from a GPA engine model as the basis for health monitoring and sensor validation in state-of-the-art engine health monitoring systems.

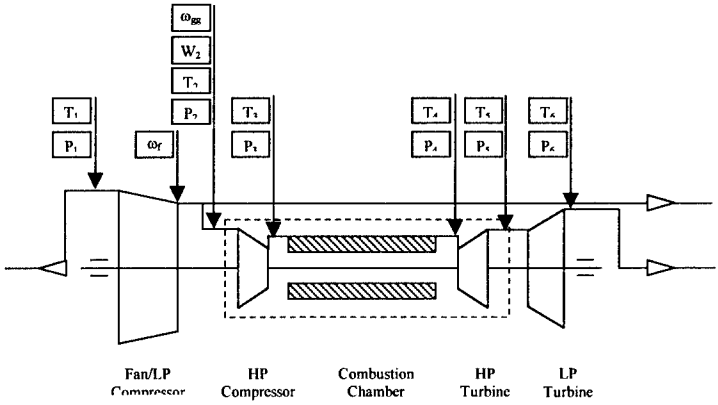

Fig. 1: Schematic of Turbofan Engine

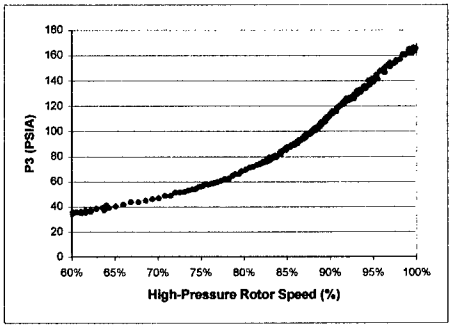

Fig. 2. Plot of P3 versus ω_{gg} for a ground test.

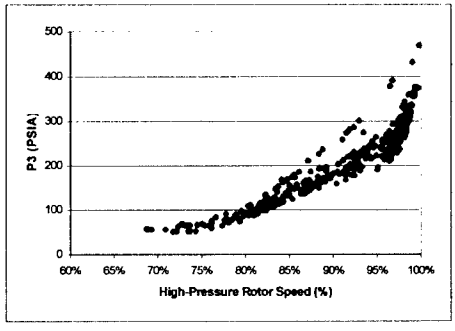

Fig. 3. Plot of P3 versus ω_{gg} for a typical mission in-flight measurement.

As analytical GPA models only cater for quasi-stationary engine operation, an alternative scheme capable of including the highly transient in-flight conditions has been developed. This lead to the formation of a diagnostic system based on parameter statistical deviations from an adaptive network-based fuzzy inference system GPA model. This is essentially a GPA model developed from a hybrid neuro-fuzzy approach based on training from typical in-flight data for a given engine. Both an overall model of the turbofan engine and models of the individual compartments have been constructed. The functional basis for the GPA models are described below.

- Transient Overall ANFIS GPA model
  The following relationship is assumed in this model. It takes transients into account by the inclusion of the low-pressure shaft speed and flow-rates. The air mass-flow is denoted by $\dot{m}_{gg}$, and the fan and gas-generator rotor speeds are denoted by ω_f, ω_{gg} respectively.

$P_n, T_n = fn(P_1, T_1, \dot{m}_{gg}, \omega_f, \omega_{gg})$ (1)

- Transient Compartmentalized ANFIS GPA model
  The following relationship is assumed in this model. It takes transients into account by the inclusion of the low-pressure shaft speed and flow-rates. Increased accuracy is obtained at the compartment level by basing output pressures and temperatures on the inlet temperatures and pressures of the compartment in question.

  $P_n, T_n = fn(P_{n-1}, T_{n-1}, \dot{m}_{gg}, \omega_f, \omega_{gg})$ (2)

  The exception to this is the modeling of T4, which would include the fuel mass flow in the model. This is an attempt to model the transients due to fuel flow variation in the combustion chamber. This would also enable the detection of abnormal fuel flow ($\dot{m}_f$) levels, and any impact to be assessed.

  $T_4 = fn(P_{n-1}, T_{n-1}, \dot{m}_{gg}, \omega_f, \omega_{gg}, \dot{m}_f)$ (3)

  P_n and T_n represent the static pressure and temperature parameters indicated in figure 1.

Figures 4 and 5 illustrate the importance of being able to have a system able to discriminate with a high degree of accuracy any deviation from normal operating conditions. The effects of high-pressure turbine efficiency drop on the deviations are shown on the parameters P_5, T_6 and P_6. Figure 4, which is based temperature and pressure deviations from a fifth-order polynomial fitting of parameters against the high pressure rotor speed, is inadequate for fault detection due to the large degree of uncertainty in measurements. In comparison, the ANFIS GPA model shrinks that uncertainty to a level that small changes in operating efficiency or capacity from normal status can be detected. Even with this improved fault resolution, it is important to use this approach in conjunction with stochastic modelling, as a relatively high degree of uncertainty will exist if individual measurements are used as the basis for assesment of the engine condition.

Figure 6 illustrates the output from the equivalent compartmentalized model for the data used in the overall model shown in figure 4. There are two major advantages that are provided by including a compartmentalized ANFIS model to complement the overall ANFIS model:

a) Increased resolution of parameters is available, as uncertainty introduced by other compartments is illuminated.
b) Ability to discriminate between the presence of single and multiple compartment faults in an engine. An overall GPA model can lead to difficulty in diagnosing the cause and mapping the progression of faults if two or more compartments are operating out of specification.

The main drawback of the compartmentalized model is that one loses the multidimensional parameter space, i.e. interaction between engine parameters, that is available in the overall model. At most two parameters, the pressure and temperature, are available in the transient ANFIS GPA model. Both methods should be incorporated to make use of the synergies that can be attained from these models. The examples illustrated are based on in-flight performance based measurements from engines without faults, which can be used to provide the baseline for generating the ANFIS GPA models. The advantage of implementing the model in the form of an adaptive network-based fuzzy inference system is that while the system can be initially formed using fuzzy sub-clustering and then trained using a hybrid neural network (least squares and backward propagation), it can be implemented as a standard fuzzy inference system.

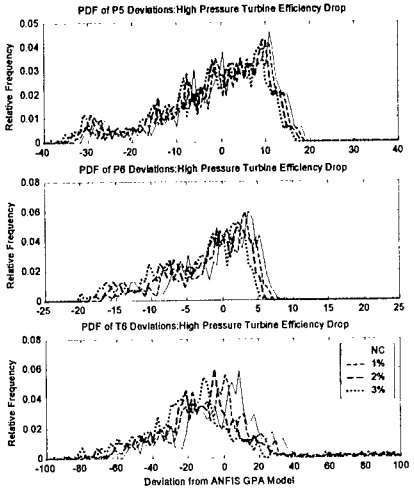

Fig. 4. PDF of deviations from fifth-order polynomial fitting $Fn(\omega_{gg})$ for in-flight missions.

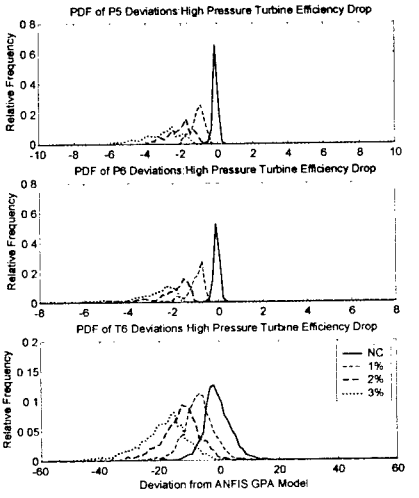

Fig. 5. PDF of deviations from overall ANFIS GPA model $Fn(P_1,T_1,\omega_{gg}, \omega_f, \dot{m}_{gg})$ for in-flight missions.

This reduces the overheads associated with deploying the system into an onboard monitoring environment, increases the operational speed of the system, and enables reasoning for the parameter deviations to be assessed.

A generic analytical GPA model was used to simulate faults in the engine, with the corresponding parameter deviations mapped onto the ANFIS model. The statistical parameter deviation database was be modeled using advanced stochastic modeling techniques to provide tools for fault detection, diagnosis and prognosis. The ability of this approach to model the deterioration of a fault statistically over time is of major benefit, as this facilitates a method for assessing the deterioration of a fault, thus providing prognostic tools that were previously extremely limited in their capabilities.

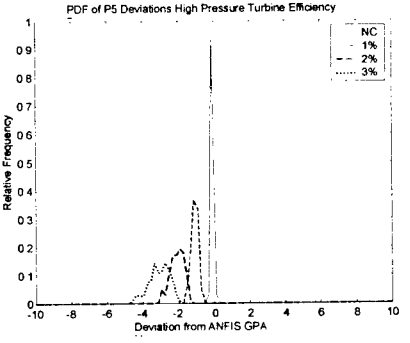

Fig. 6. PDF of deviations from compartmentalized ANFIS GPA model $Fn(P_1,T_1,\omega_{gg}, \omega_f, \dot{m}_{gg})$ for in-flight missions.

Risk-Based Fault Diagnostic and Prognostic Using GPA Model: Typically, performance parameter data measured on-line include pressures, temperatures and fuel flows in different compartments of the jet turbine engine. A pictorial representation of the proposed probabilistic fault diagnostic/prognostic procedure is given in Figure 7.

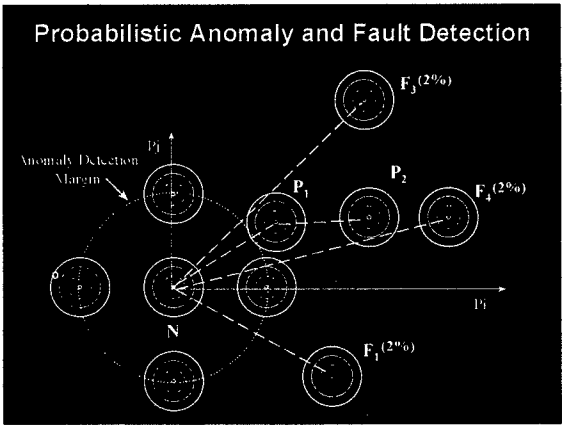

Fig. 7. Pictorial Representation of Probabilistic Fault Diagnosis Procedure

Initially, the probability distributions of measured performance parameters are defined based on statistical data acquired during normal operating conditions assuming that the turbine has no usage (represented by the origin of reference system is the multidimensional parameter space). The probability distributions of faults are defined for a given severity level in the engine efficiency loss. They are determined experimentally and/or numerically by "seeded" faults using test results and/or gas-path-analysis simulation results. During lifetime the turbine performance departs from the parameter space origin (zero bias in the measurement space) due to usage and the measured parameter probability distributions begin to shift as performance degradation occurs. After hundreds of flights when a specific anomaly detection level is reached an anomaly warning becomes active. Then, after other several hundreds of flights the measured parameter joint distribution moves to the point P1 as shown in the Figure 7. At this point, the fault looks like it might be classified with near equal probability as either a Fault 3 or a Fault 4 scenario. However, after a continued operation the measured data moves toward point P2, which will be classified with a highest degree of confidence as Fault 4. These evolutionary scenarios of turbine performance degradation shown in Figure 6, can be handled mathematically accurately by using the proposed probabilistic fault diagnostics/prognostic procedures.

Figure 8 illustrates the mean parameter deviations in five parameter spaces, such as power level, NL, pressure P3, temperatures T2 and T6 and fuel mass flow, WF, for three fault types expressed by a 2% efficiency loss. Figure 9 shows how actual engine performance Faults 1 (fan outer efficiency degradation), Fault 3 (high-pressure

compressor efficiency degradation, and Fault 4 (high-pressure turbine efficiency degradation) manifest in the parameter space.

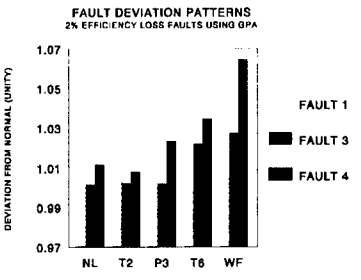

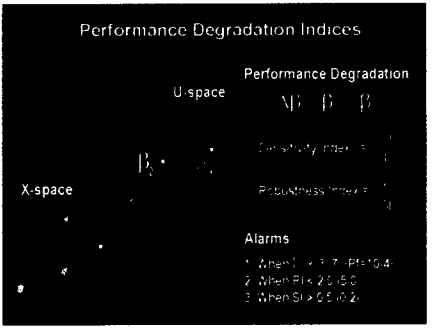

Fig. 8 Mean Deviations of Faults 1, 3 and 4 Fig. 9 Performance Degradation in U-space

The probabilistic fault diagnosis system uses as a safety margin for reliability probabilistic calculations the distance between the measured condition and the fault condition in a five-dimensional parameter space. This distance is becoming gradually smaller with respect of some faults as the performance degrades.

The turbine performance is a specific time-variant reliability problem due to usage and aging effects affecting all components. To probabilistically investigate and characterize the turbine performance evolution two types of reliability indices are introduced herein. Specifically, a cumulative and an evolutionary reliability sensitivity index for safety (performance) degradation are introduced. The cumulative reliability sensitivity index (CRSI) is defined by the "global" non-dimensional variation of the FORM reliability index, β (the relation between "failure probability", here read fault diagnostic probability, and reliability index is discussed on the next page) from initial state, at 0, to the final state, at t (over the interval [0, t]):

$$C_{0,t} = -\frac{\beta_t - \beta_0}{\beta_0} = -\frac{\Delta\beta_{ot}}{\beta_0} \tag{7}$$

The evolutionary reliability sensitivity index (ERSI) is defined by the "local" non-dimensional variation of the reliability index, from an intermediary state, at time ti, to another intermediary state, at time ti+1 (over the interval [ti, ti+1]

$$E_{ti,ti+1} = -\frac{\beta_{ti+1} - \beta_{ti}}{\beta_{ti}} = -\frac{\Delta\beta_{ti,ti+1}}{\beta_{ti}} \tag{8}$$

These two reliability sensitivity indices indicate in percents the change of the safety (performance) measure due to the time changes in the basic variables. A zero value indicates no safety (performance) degradation, while a positive value indicates a safety (performance) degradation and a negative value indicates safety improvement. Robustness indices (RI) can be defined as inverse of sensitivity indices (SI). For the engine performance degradation problem the "red" alarms can be set at a reliability index

below 3.7 (fault probability of 0.0001), for a CRSI of 0.5, or equivalently for a CRRI of 2.0 and for a ERSI of 0.2, or equivalently for a ERRI of 5.0 as shown in Figure 9.

Herein, specific quantitative measures of safety, such as safety margin, failure probability and reliability index, are used for diagnosing the faults. The conceptual framework for structural reliability and probability-based design is provided by the classical reliability theory. A general reliability model relates the "capacity" (fault conditions) and "demand" (measured conditions) variables in a limit state function (or failure equation or mode), also often called g-function of the form:

$$g(x_1, x_2, \ldots, x_n) = 0 \tag{9}$$

where $x_i, i = 1, n$ are the design variables (or life drivers). Failure occurs when $g < 0$ for any ultimate or operability (performance) limit state (or failure mode) of interest. Herein, for the engine performance reliability calculations, the failure equation is defined by the distance in the multidimensional parameter space X between a fault location, defined by vector R, and a measured usage state location, defined by vector S, i.e. g(X) = R(X) - S(X).

Then safety is assured by assigning a small probability p_f to the event that the limit state will be reached

$$p_f = \int \ldots \int f_X(x_1, x_2, \ldots, x_n) dx_1, dx_2 \ldots dx_n \tag{10}$$

in which f_X is the joint probability density function for $x_1, x_2, \ldots$, and the integration is performed over the region where $g < 0$.The failure event occurs when R - S < 0, where R is the "capacity" or "resistance' and S is the "demand" . The probability of failure is computed by

$$p_f = p(R < S) = \int_0^\infty F_R(x) f_S(x) dx \tag{11}$$

in which F_R is the cumulative probability distribution function (c.d.f.) of R and f_S is the probability density function of S. If R and S both have normal distributions the probability of failure can be computed (R-S model)

$$p_f = \Phi(-\frac{\overline{R - S}}{\sqrt{\sigma_R^2 + \sigma_S^2}}) = \Phi(-\beta) \tag{12}$$

where $\overline{R}$, σ_R are the mean and standard deviation (σ_R^2 = variance) for R and similarly for S. The function $\Phi[\ ]$ is the standard normal cumulative distribution. The notation β is the reliability index. If R and S both have lognormal distributions the failure probability can be computed (R/S model)

$$p_f \approx \Phi(-\frac{\ln(\overline{R}/\overline{S})}{\sqrt{V_R^2 + V_S^2}}) = \Phi(-\beta) \tag{13}$$

where V_R, V_S < about 0.30, in which V_R, V_S = coefficient of variation (c.o.v.) in R and S. If R and S are not normal or lognormal variables then the probability of failure can be determined using a computer algorithm.

The above equations provide a basis for quantitatively measuring structural reliability such as the measure being given by the probability of failure, p_f, or by the reliability index, β. The use of reliability index is convenient as long as the limit function is not highly nonlinear. When the limit state function is highly nonlinear the above expressions for evaluating probability of failure become crude approximations. This was the basic reason for developing the first-order reliability method, denoted FORM. While any continuous mathematical form of the limit state equation is possible, in FORM, it must be linearized at some point for purposes of performing the reliability analysis. Linearization of the failure criterion

$$Z \approx g(X_1^*, X_2^*, \ldots X_n^*) + \sum_i (X_i - X_i^*)\left(\frac{\partial g}{\partial X_i}\right)\Big|_{X_i^*} \qquad (14)$$

where $(X_1^*, X_2^*, \ldots X_n^*)$ is the linearizing point. In the classical FORM procedure, this linearizing point is obtained by computing the minimum distance between the mean point and the limit state function in a standard normal space (this distance is equal to the reliability index).

Figure 10 shows the computed turbine (reliability) performance indices, β, for the initial no-usage condition and usage conditions, P1 and P2, with respect to the Faults 1, 3 and 4. Figure 11 shows the failure probabilities computed with respect to the investigated seven fault conditions assuming initial normal condition and degraded conditions P1 and P2. It should be noted that from the start the fault diagnosis (failure) probabilities are very different for the seven faults. In the process of performance degradation these fault diagnosis probabilities may also change severely as illustrated in Figure 11. Initially, Fault 1 was the most likely fault being the closest to normal operating conditions, but after the performance degraded to condition P1 and then P2, the most likely faults have become Fault 3 and Fault 4. In the performance degradation process the turbine state departs from initial normal condition and from Faults 1, 2, 5, 6 and 7 for which the fault diagnosis probabilities become low due to direction of usage trajectories in parameter space. The evolution of the turbine performance toward Fault 4, in an opposite direction of Fault 1, is obvious from both Figures 10 and 11.

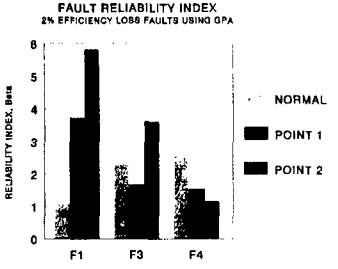

Fig. 10. Fault Reliability Index

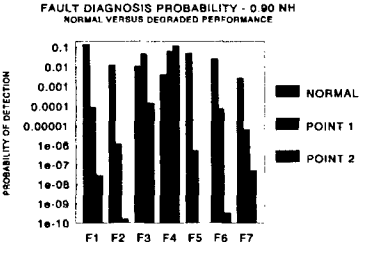

Fig. 11. Fault Probabilities

The cumulative and evolutionary reliability sensitivity indices, CRSI and ERSI, which describe the performance degradation rate in time in terms of safety indices were computed. These indices can be interpreted as Cumulative and Evolutionary Performance Degradation (RPD) index, respectively.

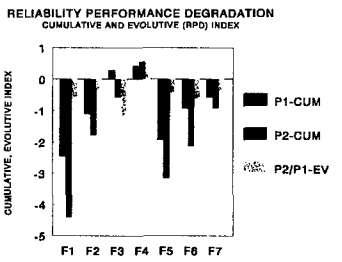

Fig. 12. Cumulative/Evolutionary Indices

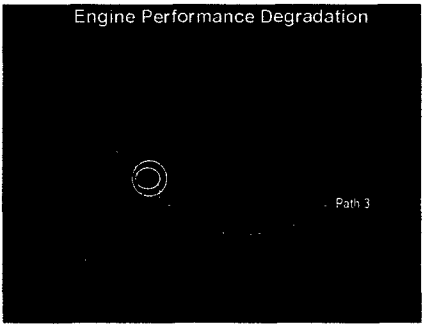

Fig. 13. Engine Performance Fault Map

Figure 12 illustrates the computed values of Cumulative RPD index for location P1 and P2, and Evolutionary RPD index for interval P1-P2. The negative values of CRPD and ERPD indicate a departure from a specific fault, while the positive values indicate a movement toward a specific fault. The CRPD and ERPD show that performance degradation was initially in the direction of Fault 3 and Fault 4 for Normal-P1 variation, and then for P1-P2 variation only in the direction of Fault 4, departing form the other six faults. The positive nature of ERPD index for Fault 4 is a decisive way to examine the movement of the measurement set in the multi-dimensional performance parameter space. The computed reliability index and the reliability sensitivity indices are used for fault diagnostic and prognostic, respectively. At instant time, depending on the fault safety margins to different faults and on the performance degradation rates in terms of safety, the remaining life of the turbine can be predicted for a given severity of efficiency loss between different times and probability levels. A minimum risk level is accepted before taking a maintenance action (in Figure 9 suggests a reliability index of 3.7).

A more realistic risk-based engine performance diagnostic-prognostic system is shown in Figure 13. The engine usage paths and faults are represented by stochastic complex trajectories and maps in multidimensional parameter space. However, this risk-based model that is currently in implementation is not discussed in this paper.

A key aspect for getting realistic results for in-flight operating conditions is to separate the *true statistical variabilities* (random part) from the *functional variabilities* introduced by engine transient behavior. For real, in-flight transient conditions the functional dependence between engine performance parameters becomes complex. If these, transient complex functional dependencies between parameters are ignored then the statistical variability is overestimated. To incorporate the complex functional dependencies for transient in-flight conditions the ANFIS has been employed.

It should be noted that important information for fault prediction is incorporated in the parameter statistical deviations after ANFIS was applied. These statistical deviations are not noises. The multiple-parameter statistical deviations can be described using a multidimensional stochastic process model. Figure 14 shows auto- and cross-correlation functions for different pair of parameters for normal conditions and fault conditions. For fault conditions the correlation length of parameter deviations is larger than for normal operating conditions.

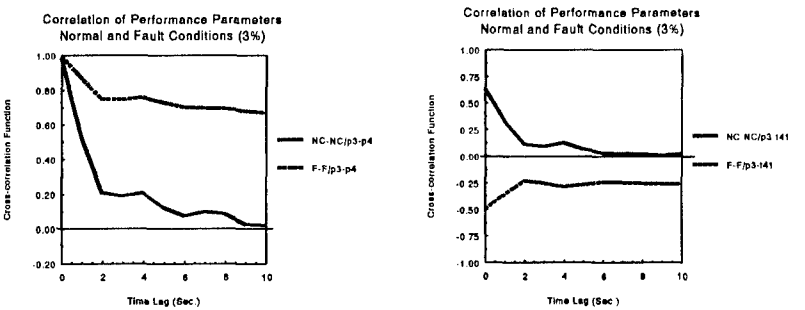

Figure 15: Correlation of Performance Parameters

The zero-time lag cross-correlation estimations between different performance parameters are incorporated in probabilistic fault diagnostic model.

Concluding Remarks:

The conceptual framework for a Probabilistic *Prognostic Health Management* (PHM) system has been outlined. The proposed *Stochastic-Fuzzy-Inference Model-Based System (StoFIS)* has been demonstrated to be capable of performing accurately under highly transient in-flight conditions, as encountered during military operations, through the exploitation of an ANFIS based GPA model. Probabilistic tools then enable deviations from the model to be used for risk-based fault diagnostics and prognostics.

References:

[1] Altmann J., Mathew J. "Automated DWPA Feature Extraction of Fault Information from Low Speed Rolling-Element Bearings", Proceedings of Asia-Pacific Vibration Conference, Singapore, 1999

[2] Ghiocel, D.M., "Advanced Stochastic Classifiers for Jet Engine Performance and Vibration", 55th MFPT Conference, Virginia Beach, NC, May 4-6, 2000

[3] Ghiocel, D. M., Roemer, M J. "A New Probabilistic Risk-Based Fault Diagnosis Procedure for Gas Turbine Engine Components" 40th AIAA/ASME/ASCE/AHS/ASC Non-Deterministic Approaches Forum, St. Louis, MO, April 12-15, 1999